SANDIA REPORT

SAND2007-6190

Unlimited Release

Printed October 2007

Controlled Fabrication of Nanowire Sensors

François Léonard

Prepared by
Sandia National Laboratories
Albuquerque, New Mexico 87185 and Livermore, California 94550

Sandia is a multiprogram laboratory operated by Sandia Corporation,
a Lockheed Martin Company, for the United States Department of Energy's
National Nuclear Security Administration under Contract DE-AC04-94AL85000.

Issued by Sandia National Laboratories, operated for the United States Department of Energy by Sandia Corporation.

Available to DOE and DOE contractors from
U.S. Department of Energy
Office of Scientific and Technical Information
P.O. Box 62
Oak Ridge, TN 37831

Telephone: (865) 576-8401
Facsimile: (865) 576-5728
E-Mail: reports@adonis.osti.gov
Online ordering: http://www.osti.gov/bridge

Available to the public from
U.S. Department of Commerce
National Technical Information Service
5285 Port Royal Rd.
Springfield, VA 22161

Telephone: (800) 553-6847
Facsimile: (703) 605-6900
E-Mail: orders@ntis.fedworld.gov
Online order: http://www.ntis.gov/help/ordermethods.asp?loc=7-4-0#online

SAND2007-6190
Unlimited Release
Printed October 2007

Controlled Fabrication of Nanowire Sensors

François Léonard
Materials Physics Department
Sandia National Laboratories
Livermore, CA 94551

Abstract

We present a simple top down approach based on nanoimprint lithography to create dense arrays of silicon nanowires over large areas. Metallic contacts to the nanowires and a bottom gate allow the operation of the array as a field-effect transistor with very large on/off ratios. When exposed to ammonia gas or cyclohexane solutions containing nitrobenzene or phenol, the threshold voltage of the field-effect transistor is shifted, a signature of charge transfer between the analytes and the nanowires. The threshold voltage shift is proportional to the Hammett parameter and the concentration of the nitrobenzene and phenol analytes. For the liquid analytes considered, we find binding energies of 400 meV, indicating strong physisorption. Such values of the binding energies are ideal for stable and reusable sensors.

THIS PAGE INTENTIONALLY BLANK

CONTENTS

FIGURES

This Page Intentionally Blank

1. Introduction

Nanowires made up of elemental, compound, and metal-oxide semiconductor materials have emerged as promising elements for chemical and biological sensing, with proof-of-principle devices demonstrated for detection of various gases[1,2,3], pH in aqueous media[4], antibody binding,[4] and DNA hybridization[5] . The high surface-to-volume ratio of nanowires, coupled with diameter dimensions that are comparable to the Debye length result in a strong dependence of carrier concentration on the surface charge density. Thus, processes such as protonation/deprotonation or adsorption/desorption which modify the surface charge density lead directly to measurable changes in nanowire conductance. Silicon nanowires (SiNWs) are particularly appealing for sensing applications, since the Si oxide can effectively passivate surface dangling bonds, and at the same time can be chemically modified through the well known silanol chemistry to provide surface functionalization and, therefore, selectivity for particular analytes. To date, most nanowire-based devices including sensors were fabricated by a labor intensive sequence of steps that included nanowire synthesis and dispersion followed by direct-write lithography and metallization, resulting in one or a few selected specimens.[6] Top-down techniques based on electron beam lithography to define individual SiNWs on silicon-on-insulator substrates have also been demonstrated[7]. Alternative approaches to large scale nanowire integration such as electric field directed deposition[8],[9] or fluidic assembly[10] are promising, but still present formidable challenges, such as lack of long range control and poor contact quality, since nanowires are often deposited *on top* of prefabricated electrodes, where adsorbed organics or moisture often introduce additional and difficult-to-reproduce contact resistance. Furthermore, vapor-liquid-solid (VLS), laser ablation, or chemically synthesized nanowires often exhibit a substantial variation in diameter, which can introduce an undesirable spread in the electrical response of nanowires to analyte gases.[6,11]

Here, we demonstrate a simple, top-down technique based on nanoimprint lithography (NIL) to define SiNWs over a large area and with high density and uniformity. While NIL has been used recently to create metallic nanowires[12], its use for SiNWs has not been reported; and regardless of the fabrication method, large area, dense arrays of perfectly ordered SiNWs have not been investigated for sensing.

Invented in the mid 1990's, NIL transfers the etched patterns from a mold (or template) into a thermoplastic or a photocurable polymer through direct contact instead of through optical systems.[13,14] Unencumbered by diffraction limitations, NIL does not require expensive light sources or optics that hinders photolithography and has achieved sub-100 nm resolution at a much lower cost. NIL is particularly well suited for simple, one-mask level patterns that have to be defined over large area and with nanometer scale critical dimensions.

In this letter, we use NIL to pattern the device layer of a silicon-on-insulator (SOI) substrate into 75 nm wide silicon nanowires that span the entire 100 mm diameter wafer, and with a density of 5 SiNWs/□m. We measure the transport and transistor characteristics of these nanowires, and demonstrate their application to chemical sensing using ammonia gas and liquid solutions of nitrobenzene and phenol in cyclohexane. Analysis of the results indicates that the sensing mechanism is charge transfer between the analytes and the nanowires, and scales with the value of the Hammett parameter for the organic solutions.

2. Device Fabrication

A boron doped (10-20 ohm-cm) SOI wafer with a 100 nm thick device layer and a 155 nm buried oxide layer was purchased from Silicon Quest Inc. The wafer was thermally imprinted using a Nanonex 2000 NIL tool[15], using a 200 nm dense pitch (100 nm line/space) Si grating mold. The resulting pattern was transferred into the underlying SOI device layer using reactive ion etching with Cl_2/HBr plasma. SEM images of the individually addressable Al electrodes over the SiNWs are shown in Fig. 1(a) and 1(b), while cross sections at 60^o and 90^o with respect to the plane of the figure are shown in Figures 1(c) and 1(d). The SEM images clearly demonstrate the uniformity of the NIL fabricated SiNWs. Similar images to the one shown in Fig. 1(b) collected from different locations across the wafer were used to determine average line width and line edge roughness values. Analysis using the GORA[14] digital image analysis program yielded an average SiNW diameter of 76 ± 5 nm with an LER of 5 nm. The variability of only 6 percent in diameter is likely due to variations in the original mold (which itself is a replicate of an original mold fabricated by laser interference lithography), coupled to non-uniformity in the reactive ion etching.

To form source and drain contacts, arrays of interdigitated Al electrodes, 180 μm long, 1 μm to 2 μm wide, and with inter-electrode spacing of 1 μm, 2 μm, and 4 μm were defined over

the SiNWs using optical lithography followed by electron beam evaporation and lift-off. Each Al electrode array consisted of 32 individually addressable, parallel contacts, with ~ 900 SiNWs spanning the gap between any pair of electrodes. The metallized wafer was then annealed in vacuum at 450°C for 20 min to render the Al contacts ohmic, and exposed to O_2 plasma to remove residual organics and ensure that the nanowire surface was clean and oxidized.

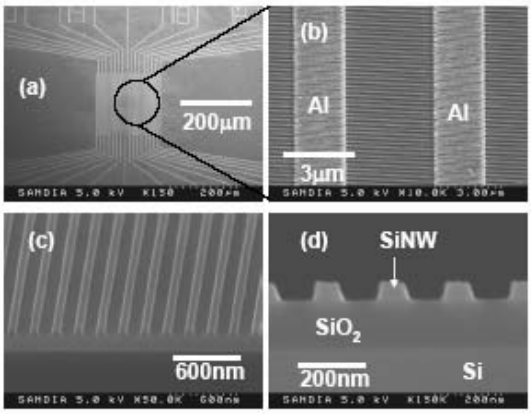

Figure 1. Top-down image of one SiNW device showing the interdigitated Al source-drain electrodes. (b) Close-up image of SiNWs between two Al electrodes. (c), (d) cross section SEM images of SiNWs at 60° and 90° tilt with respect to the plane of the figure.

3. Electrical characterization

Electrical characterization of the SiNWs was performed using a HP model 4145B semiconductor parameter analyzer connected to a micromanipulator probe station. The p-doped Si bottom (handle) portion of the SOI wafer was used as the gate electrode, with an In ohmic bottom contact. A family of gate voltage sweeps, I_{SD}-V_g, collected at V_{SD}=1.0 Volts for different Al electrode pairs for a selected interdigitated array is shown in Fig. 2. The I_{SD}-V_g curves correspond to three regimes: hole accumulation (regime I), intrinsic or 'off' (regime II), and electron accumulation (regime III), as indicated by the three band diagrams in the figure. (We believe that the contacts are heavily p-doped as a result of Al diffusion during the contact formation process.) The I_{SD}-V_{SD} behavior of the device in the hole accumulation regime shows behavior similar to p-channel MOSFETs, as indicated in Fig. 2b.

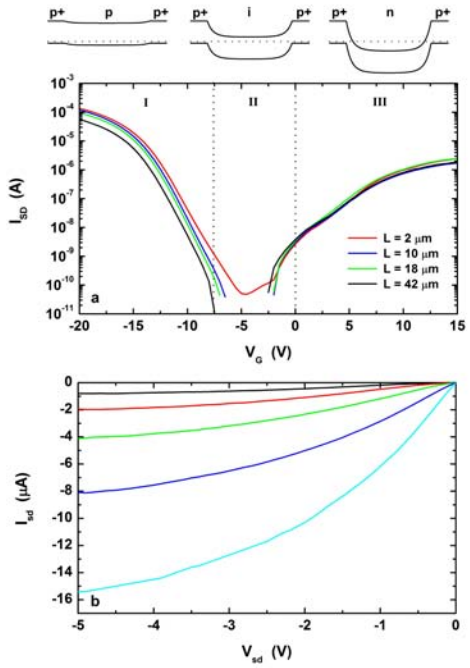

Figure 2: (a) I_{SD} versus V_g for one SiNW device collected for different Al electrode pairs on the same array and with V_{SD} set at 1 Volt. (b) I_{SD} versus V_{SD} for a different SiNW device. Curves from top to bottom correspond to gate voltages of -10, -11, -12, -13 and -14 Volts.

The transport behavior can be examined by plotting the resistance of the device of Fig. 2a as a function of nanowires length (i.e. for different pairs of electrodes) in the hole accumulation regime. This is shown in Fig. 3, indicating that the resistance scales linearly with nanowires length, and thus that the transport is diffusive. Analysis of the I_{SD}-V_g characteristics using a standard transistor diffusion model gives a threshold voltage of -15.81 V, and a mobility of 81 cm^2/Vs. This value for the mobility is somewhat lower than that in bulk silicon, and more work is needed to elucidate the origin of this effect. Scattering with the nanowire surface, contact resistance or conductivity through a partial cross-section of the nanowires are possible reasons for the reduced mobility.

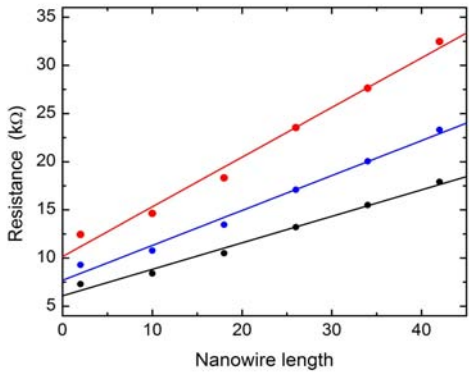

Figure 3: Resistance of the nanowire array of Fig. 2a as a function of nanowires length. Curves from top to bottom correspond to gate voltages of -18, -19 and -20 V.

4. Chemical Sensing

To explore the chemical sensing characteristics of the NIL-based SiNWs we chose to first test the device sensitivity to ammonia vapor, NH_3, by exposing one SiNW array to vapor from an ammonium hydroxide solution[16]. Ammonia is well known to be a strong reducing agent and its effect on transistor characteristics of carbon nanotube devices in air is to make the threshold voltage more negative (i.e. ammonia acts as an additional positive gate bias).[17] Figure 4 indicates that similar behavior is observed for the SiNW sensors described in this letter, where the I_{SD}-V_g curves are shifted to the left for both the hole and electron accumulation regimes.

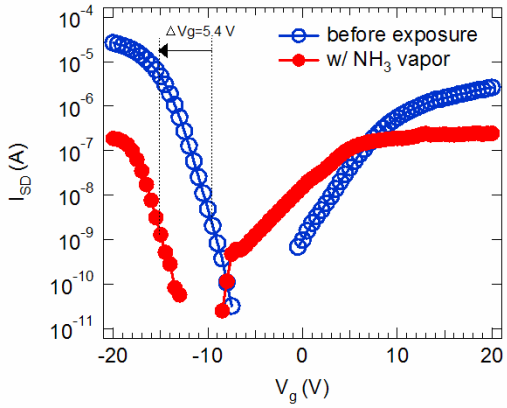

Figure 4: Variation in I_{SD} versus V_g for a SiNW array exposed to ammonia vapor from an ammonium hydroxide solution. The indicated ΔV_g of 5.4V is determined for $I_{SD}= 10^{-9}$A.

To explore the sensing characteristics of the SiNWs in a more quantitative manner, we measured the effect of different concentrations of nitrobenzene and phenol in cyclohexane solutions on the device electrical characteristics. Nitrobenzene and phenol are electron withdrawing and electron donating molecules, respectively, and their solution in cyclohexane have previously been used to change the I_{SD}-V_g characteristics of carbon nanotube transistors.[18] Solutions of nitrobenzene and phenol in cyclohexane with

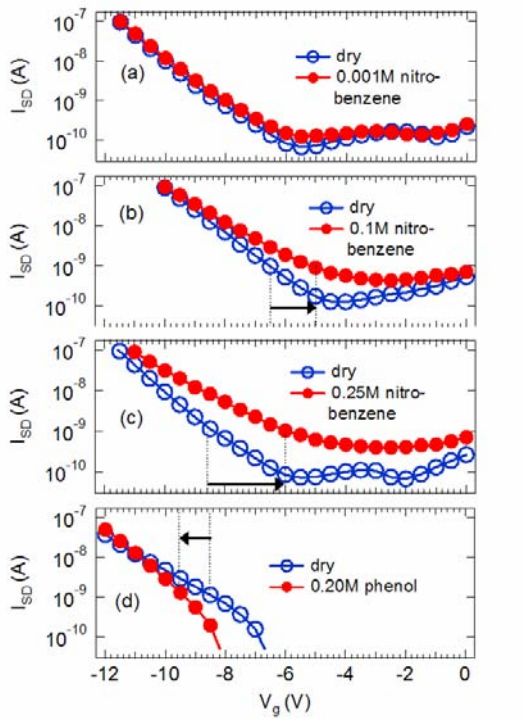

Figure 5: Variation in I_{SD} versus V_g for (a) 0.001M, (b) 0.1M, and (c) 0.25M concentrations of nitrobenzene dissolved in cyclohexane and applied directly over the SiNW array sensor. Panel (d) shows the variation when the device is exposed to 0.2M phenol in cyclohexane.

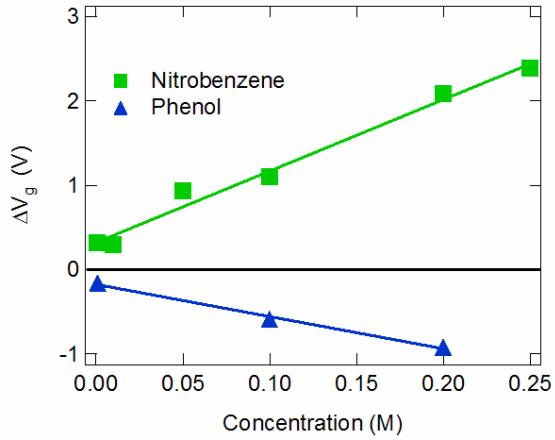

Figure 6: Shift in V_g necessary to maintain I_{SD}=1 nA in accumulation mode as a function of the solute concentration in cyclohexane.

concentrations ranging from 0.001M to 0.25M were applied using a micro-pipette directly over one of the SiNWs devices, while I_{SD}-V_g curves were measured just before and just after the solution application. The resulting curves for three of the concentrations of nitrobenzene are shown in Fig. 5, where it can be seen that the effect of nitrobenzene is to increase the drain current for a given gate bias in the accumulation regime. The increase in I_{SD} is consistent with the electron withdrawing character of nitrobenzene, as it effectively dopes the

SiNWs p-type. Figure 5 shows that the shift in I_{SD}-V_g curves is sensitive to the nitrobenzene concentration. This is further highlighted in Fig. 4, where the change in gate bias corresponding to I_{SD} of 1 nA is plotted as a function of the nitrobenzene concentration, indicating a linear behavior. Also included in Fig. 5 is the effect of 0.20M phenol solution on a similar SiNW device, where the shift is opposite that of nitrobenzene, and consistent with the shift observed for ammonia gas. To provide a rough estimate of reproducibility in electrical response, three separate measurements were carried out for the concentration of 0.20M nitrobenzene, with the device rinsed in pure cyclohexane between each measurement, yielding an average shift of V_g =2.10±0.15V.

5. Theory

To understand the sensing characteristics of the nanowire array we consider the adsorption of the molecules on the nanowires surface, the associated charge transfer and its effect on the threshold voltage. The change in the threshold voltage is related to the charge transferred to the nanowires as

$$\Delta V_g = C^{-1}\Delta Q \qquad (1)$$

where ΔQ is the charge per NW, and C is the capacitance of the NW array, given by $C = 2\pi\varepsilon L / \left[2\Sigma_{n=1}^{N} \ln\left(2\sqrt{h^2 + n^2 l^2}\,/\,r\right) + \ln(2h/r)\right]$ with L the NW length, N the number of NWs, r the NW radius, h the gate thickness, l the spacing between nanowires, and ε the gate dielectric constant. The charge on a NW is related to the surface coverage θ through the relation

$$\Delta Q = 6rLe\lambda a^{-1}\theta \qquad (2)$$

where a is the area that a molecule occupies on the surface and λ is a parameter that denotes the fraction of electronic charge transferred to the NW per molecule.

To relate θ to the analyte concentration in the liquid, we consider equilibrium between the liquid and the surface, with the partition function[19]

$$Z = 1 + z_{vib} e^{(\mu - E_b)/kT} \qquad (3)$$

where μ is the chemical potential of the analyte in the liquid, E_b is the binding energy of the molecule to the surface and z_{vib} is the contribution to the partition function due to vibrations. The chemical potential is obtained from the expression $\mu = \mu_0 + kT \ln x$ where μ_0 is the chemical

potential of the pure substance and x is the mole fraction. Since for a pure substance the chemical potential is simply equal to the Gibbs free energy, μ_0 can be calculated from $\mu_0 = \Delta H_f - TS$ where ΔH_f is the enthalpy of formation and S is the entropy.

Assuming that the mole fraction of the solute is much less than the solvent, we obtain the equilibrium surface coverage as a function of the solute concentration

$$\theta = \frac{c}{c + c_0} \qquad (4)$$

where

$$c_0 = \bar{c} z_{vib}^{-1} e^{-\mu_0 / kT} e^{E_b / kT} \qquad (5)$$

with $\bar{c}$ the solvent concentration. For $c << c_0$, Eqs (1), (2) and (4) give

$$\Delta V_g = \frac{6rLe\lambda}{Cac_0} c. \qquad (6)$$

A least-squares fit to the data of Fig. 6 for nitrobenzene gives a value for the prefactor of 8.47±0.53 V/M. Using Eqs (5) and (6), a value of μ_0 of -0.56 eV and assuming λ=1 and z_{vib}=1 we obtain a value for the binding energy of 440 meV. This value indicates strong physisorption of the nitrobenzene on the NW surface. The fact that $E_b >> kT$ explains why our devices are very stable once exposed to the analytes. But just as important, the binding energy is much less than chemisorption binding energies, and thus provides the opportunity to refresh the device, as our simple pure cyclohexane rinse has demonstrated.

From the above calculations, the value of c_0 is 770 M; thus for any practical purpose the coverage is linear with concentration, leading to the linear dependence of the voltage shift observed in Fig. 6. This linear dependence is important to allow for a quantitative determination of the solute concentration. From the relation $\theta = c/770M$ we estimate the density of molecules on the NW surface at 0.25M to be 0.3 molecules/nm/NW. This small density is also consistent with the linear behavior of Fig. 6.

For phenol, the least-squares fit gives a value for the prefactor of -3.56±0.61 V/M. This behavior is consistent with the electron donating properties of phenol, which causes a shift of the gate voltage in the negative direction. Previous work on the sensing properties of

carbon nanotubes[14] has shown that the voltage shift is proportional to the Hammet parameter σ_p. For nitrobenzene, $\sigma_p = 0.78$ while for phenol $\sigma_p = -0.4$; the ratio ~ -2 is in reasonable agreement with the ratio of the slopes from Fig. 6 equal to -2.4.

Acknowledgements

This work was performed under the Laboratory Directed Research and Development program at Sandia National Laboratories.

References

[1] Xia Y.; Yang, P.; Sun, Y.; Wu, Y.; Mayers, B.; Gates, B.; Yin, Y.; Kim, F.; Yan, H. *Advanced Materials* **2003**, 15, 353
[2] Fan, Z.; Lu, J. G. *Appl. Phys. Lett.* **2005**, 86, 123510-1
[3] Comini, E.; Faglia, G.; Sberveglier, G.; Pan, Z., Wang, Z. L. *Appl. Phys. Lett.* **2003**, 81, 1869
[4] Cui, Y.; Wei, Z.; Park, H.; Lieber, C. M. *Science* **2001**, 293, 1289
[5] Li, Z.; Chen, Y.; Li, X.; Kamins, T. I.; Nauka, K.; Williams, R. S. *Nano Lett.* **2004**, 4, 245
[6] Cui, Y.; Duan, X.; Huang, Y., Lieber, C. M. in *Nanowires and Nanobelts Materials, Properties, and Devices, Volume 1: Metal and Semiconductor Nanowires*, Wang, Z. L. Ed.; Kluwer: Boston, **2003**.
[7] Koo, S-M.; Edelstein, M. D.; Li, Q.; Richter, C. A.; Vogel, E. M. *Nanotechnology* **2005**, 16, 1482.
[8] Léonard, F.; Jones, F. E.; Talin, A. A.; Dentinger, P. M. *Appl. Phys. Lett.* **2005**, 86, 093112
[9] Lao, C. S.; Liu, J.; Gao, P.; Zhang, L.; Davidovic, D.; Tummala, R.; Wang, Z. L. *Nano Lett.* **2006**, 6, 263
[10] Patolsky, F.; Lieber, C. M. *Materials Today*, **2005**, April, 20.
[11] Cui, Y.; Lauhon, L. J.; Gudiksen, M. S.; Wang, J.; Lieber, C. M. *Appl. Phys. Lett.* **2001**, 78, 2214
[12] Jung, G. Y.; Wu, W.; Ganapathiappan, N.; Ohlberg, D. A. A.; Islam, M. S.; Li, X.; Olynick, D. L.; Lee, H.; Chen, Y.; Wang, S. Y.; Tong, W. M.; Williams, R. S.; *Appl. Phys. A* **2005**, 81, 1331.
[13] Chou, S. Y.; Krauss P. R.; Zhang, W.; Guo, L. J.; Zhuang, L. *J. Vac. Sci. Technol. B* **1997** 15 2897
[14] Chou, S. Y. in *Alternative Lithography,* Sotomayor, T. S. Ed., Kluwer: Boston, **2003**
[15] Further information about the Nanonex NIL tools and the imprint process can be obtained from the Nanonex web site: www.nanonex.com
[14]GORA © , a digital image analysis program for line edge roughness and line width measurements, is copywritten software, ©1999 Sandia National Laboratories
[16] A small cotton applicator stick was soaked in 8M ammonium hydroxide solution and placed several inches from a SiNW array under test.
[17] Bradley, K.; Gabriel, J-C. P.; Briman, M.; Star, A.; Gruner, G.; *Phys. Rev. Lett.* **2003**, 91, 218301-1
[18] Star, A.; Han, T-R.; Gabriel, J-P. P.; Bradley, K.; Gruner, G. *Nano Lett.* **2003**, 3, 1421
[19] Blakeley, J. M.; Shelton, J. C. in *Surface Physics of Materials*, Blakeley, J. M. Ed.; Academic Press: New York, **1975**.

Distribution List

Internal

SNL/CA

1	MS 9042	Tony Chen	08776
1	MS 9161	Sarah Allendorf	08756
1	MS 9161	Art Pontau	08750
1	MS 9292	Blake Simmons	08755
1	MS 9402	Rion Causey	08758
1	MS 9402	John Goldsmith	08772
1	MS 9403	Timothy Shepodd	08778
1	MS 9405	Bob Carling	08700
1	MS 9409	Chris Moen	08757
2	MS 9018	Central Technical Files	8944
2	MS 0899	Technical Library	9536
1	MS 0123	D. Chavez, LDRD Office	1011


Sandia National Laboratories